Unexpected bell-shaped double layer capacitance promoted by nitrate anions at a-CNx / aqueous electrolyte interface and simulated with the lattice-gas model

Nathalie Simon, Catherine Debiemme-Chouvy, Florence Billon, Hubert Cachet

Unexpected bell-shaped double layer capacitance promoted by nitrate anions at a-CNx / aqueous electrolyte interface and simulated with the lattice-gas model

Nathalie SIMON , Catherine DEBIEMME-CHOUVY , Florence BILLON , Hubert CACHET

PII: S0013-4686(24)01402-6
DOI: https://doi.org/10.1016/j.electacta.2024.145165
Reference: EA 145165

To appear in: *Electrochimica Acta*

Received date: 4 July 2024
Revised date: 5 September 2024
Accepted date: 27 September 2024

Please cite this article as: Nathalie SIMON , Catherine DEBIEMME-CHOUVY , Florence BILLON , Hubert CACHET , Unexpected bell-shaped double layer capacitance promoted by nitrate anions at a-CNx / aqueous electrolyte interface and simulated with the lattice-gas model, *Electrochimica Acta* (2024), doi: https://doi.org/10.1016/j.electacta.2024.145165

Unexpected bell-shaped double layer capacitance promoted by nitrate anions at a-CNx / aqueous electrolyte interface and simulated with the lattice-gas model

Nathalie SIMON[1,2], Catherine DEBIEMME-CHOUVY[1], Florence BILLON[1], Hubert CACHET[1]

[1] *Sorbonne Université, CNRS, Laboratoire Interfaces et Systèmes Electrochimiques, LISE, UMR 8235, F-75005 Paris, France*

[2] *Université Paris-Saclay, UVSQ, CNRS, Institut Lavoisier de Versailles, UMR 8180, F-78000 Versailles, France*

Corresponding Author:
Catherine Debiemme-Chouvy
E-mail: catherine.debiemme-chouvy@sorbonne-universite.fr

ABSTRACT

Amorphous carbon nitride thin fims, a-CN_x, are potentially low cost candidates for electrochemical nitrate treatment by comparison to boron doped diamond electrodes. In aqueous media, a-CN_x electrodes are characterized by a large potential window and, in acidic pH solutions, no surface charge capacitive contribution. In perchloric acid at pH 1, nitrate reduction occurs at the negative limit of a potential domain without any significant redox reaction over almost 1 Volt. In this domain, in the presence of a nitrate salt, a bell-shaped behaviour was observed for the interfacial capacitance. Differences were evidenced according to the solvation state of the cations (Na^+, K^+, Li^+, Cs^+, $(CH_3)_4N^+$, $(C_2H_5)_4N^+$), depending on the cation size. Experimental capacitance data were simulated by using the phenomenological theory developed by Kornyshev in the case of ionic liquids. A good agreement was obtained assuming a compact layer in series with the highly structured diffuse layer and taking into account the short-range ion-ion interactions. Thus, at the a-CNx/aqueous electrolyte interface, nitrate anions are engaged into strong anion-cation interactions (ion pairing) especially with small sized cations, leading to nitrate anion trapping in the multilayered interfacial region with a possible negative effect on the nitrate ions electroreduction.

INTRODUCTION

Many methods have been proposed to reduce the amount of nitrate ions in the environment: among them, ion-echange or biofiltration[1], the electrocatalytic reduction with H_2 [2], have been envisaged with specific merits or drawbacks concerning the selectivity towards reaction products or the costs of the treatments.

Though thermodynamics data indicate a rather easy reducibility of nitrates with relatively high standard potentials, the actual overpotentials for several reactions concerning the reduction of nitrate and those of some of its reaction products are quite negative and thus the associated reduction waves are often masked by the hydrogen evolution reaction on metallic electrodes. There are metallic materials which present a more catalytic ability, such as copper, but the potential range where nitrate reduction occurs also corresponds to corrosion conditions and is badly appropriate with a view to application.

Some years ago, the electrochemical route has received a new impulse with the boron-doped diamond (BDD) films and more generally with the diamond-like-carbon (DLC) materials, which have emerged as promising new electrode materials in electrochemistry in view of their wide available potential window in aqueous electrolytes.[3]

Several kinetics investigations on nitrate electroreduction with BDD electrode have been carried out.[4,5,6,7] From a practical point of view, the drawback of BDD electrodes is their fabrication cost, it is not so much the case for DLC materials like a-CN_xH_y or a-CN_x thin films. In a recent past, we have elaborated such nitrogen-incorporated hydrogenated[8] or not [9] [10] [11] amorphous thin films with very similar performances as BDD with respect to both wide potential window in water and electrochemical reactivity towards outer sphere redox reactions as for instance the ferri/ferrocyanide system ($[Fe(CN)_6]^{3-/4-}$). Electrochemical impedance spectrosopy (EIS) is a valuable tool to get information on the organization of the electrode/electrolyte interfacial region *via* the determination of the interfacial capacitance and its potential dependence. Many physical effects are able to contribute to the capacitance, such as the electrode surface roughness, the type of solvent medium (polar solvent or ionic liquid), surface charge modification arising from electrolyte/electrode interactions *via* chemical or electrochemical routes. It means that the resulting information taken out from capacitance measurements will strongly depend on the experimental conditions.

Contrary to liquid metal as mercury[12], a non purely capacitive behavior is unavoidable in the case of solid electrode material.[13,14,15] Classically, frequency dispersion of capacitance is formally characterized by a Constant Phase Element (CPE), the origin of which being the local inhomogeneities either normal to or along the electrode surface. Face with these constraints, we select a-$CN_{0.13}$ thin film as an electrode material offering an inert surface chemistry in a dedicated

aqueous electrolyte and, when deposited on silicon single crystal, is characterized by a very low surface roughness at the atomic scale in favour of a low capacitance frequency dispersion. Another advantage was to optimize the experimental conditions to study the structural organisation of the interfacial region, knowing that the water structure itself and the ion distribution may be influenced by the electrode roughness.[16]

The present work is focused on the examination of the potential profile of the interfacial capacitance of a-$CN_{0.13}$ thin film electrode in the presence of nitrates during cathodic polarisation. The first stages of nitrate reduction in acidic aqueous solution was investigated at a pH value for which there is no surface charge capacitance contribution. It was found that the electrochemical response was influenced by the type of cation in the electrolyte. It was observed that nitrate reduction takes place at the negative limit of a large potential window free of any transfer reaction allowing the examination of the potential dependence of the interfacial capacitance from which structural information can be gained. The main finding was an unexpected bell-shaped behaviour induced by the presence of nitrate anions. Capacitance data were completed by varying the cation partner of the nitrate anion or the concentration of the nitrate salt. These capacitance data have been analyzed within the frame of the formalism developed by Kornyshev for ionic liquids [17,18,19,20,21,22,23], supplying the theoretical tools for a direct quantitative interpretation of the capacitance profiles. From this comparison, it is demonstrated that strong nitrate-cation interactions take place in the interfacial layer, able to influence the reduction potential and to hamper the transfer reaction by trapping ion in the diffuse layer.

EXPERIMENTAL CONDITIONS

a-CNx elaboration and electrochemical set-up

a-CN_x thin films were elaborated by DC magnetron sputtering from a graphite target in the presence of a reactive argon plasma containing nitrogen at 3%, using a MP 300 S reactor from PLASSYS company (France). The total gas pressure was 1 Pa therefore the partial nitrogen pressure was set at 0.03 Pa, which corresponds to x = 0.13 according to our previous works.[24] The films were deposited onto highly doped Si(100) single crystal silicon substrates (doping level: 10^{18} cm^{-3}) cut as 1 cm^2 squares. The electrodes were laterally isolated by epoxy resin leaving a square-shaped active surface area of 0.4 cm^2. These amorphous a-CNx films with thickness about 400 nm are pinhole-free, chemically inert, and have a surface roughness at the nanometer scale.[24]

They were used in a classical three-electrode cell arrangement, under argon atmosphere, with a counter electrode made of a platinum grid of large area and a calomel reference electrode saturated with KCl (SCE). The a-$CN_{0.13}$ electrodes were electrochemically pre-treated by cycling (50 $mV \cdot s^{-1}$) 15 times in $HClO_4$ 0.5 M between +1 to -1.5 V/SCE. Moreover before each electrochemical

measurement (voltammetry and EIS), in order to obtain reproducible electrode surface, two successive anodic pulses were performed at +1.5 V/SCE for 5 s, resulting in an instantaneous anodic current of about 10 $\mu A \cdot cm^{-2}$.

The electrochemical interface for voltammetry and EIS was a GAMRY 600+. EIS data analyses were performed using the home-made SIMAD software, according to an equivalent electrical circuit already proposed in previous works[9] and depicted in **Figure 1A**. It is composed with two resistance-capacitance parallel combinations in series with the electrolyte resistance, R_{el}. The circuit labelled (R_{Si}, C_{Si}) corresponds to a degeneracy of the silicon/carbon interface or to a superficial insertion into Si of carbon and/or nitrogen atoms at the beginning of the film growth.[25] This contribution takes place at frequencies higher than a few kHz and is found to be independent of the dc potential and well separated from the interfacial response. The second part of the circuit represents the interfacial impedance, with the double layer capacitance, C_{dl}, formally represented by a CPE element, Q_{dl}, in parallel with the transfer resistance, R_t. The CPE element, classically defined as an impedance $Z_{CPE} = 1/(Q_{dl}.(j\omega)^n)$, was considered to account for the residual non ideal behaviour of the interfacial capacitance, in agreement with the very low surface roughness of the a-CNx electrode deposited on a silicon single crystal. It was found that for all the EIS data obtained in this work the CPE exponent, n, was very close to 1, allowing to apply the Brug procedure[26] to reach the true C_{dl} capacitance :

$$C_{dl} = (\frac{1}{R}).(R.Q_{dl})^{\frac{4}{n}} \quad (1)$$

with $1/R = 1/(R_{Si}+R_{el}) + 1/R_t$

All the experiments were conducted in $HClO_4$ 0.1 M solution, because at such acidic pH there is no significant contribution of the surface charge due to amine and/or imine groups located at the a-CNx surface.[9]

Different solutions were prepared in $HClO_4$ 0.1 M by adding various amounts of $LiClO_4$, $NaClO_4$, $LiNO_3$, $NaNO_3$, KNO_3, $CsNO_3$, $tMeNO_3$ or $tEtNO_3$ salts ; tMe and tEt stand for tetra methyl ammonium, $(CH_3)_4N^+$, and tetra ethyl ammonium, $(C_2H_5)_4N^+$, cations, respectively. For each studied solution, eighteen EIS spectra from 0.6 Hz to 70 kHz with five points per frequency decade were recorded between -0.40 to -1.25 V/SCE by step of 50 mV and analyzed as indicated above to produce the corresponding C_{dl}(E) curve. This potential window was chosen to be essentially outside the nitrate reduction reaction, as justified below by voltammetry. A typical example of all the impedance spectra recorded in the present work is depicted in **Figure 1** for the a-$CN_{0.13}$/($HClO_4$ 0.1 M + $NaNO_3$ 0.01 M) system, as Nyquist plot (**Figure 1B** and **1C**) or Bode plot (**Figure 1D** and **1E**). The two capacitive loops of the equivalent circuit (**Figure 1A**) are clearly evidenced in both

representations. The high frequency (HF) loop due to the interface between the a-CN_x film and the Si substrate is located in the kHz range and quasi-independent on the dc polarization potential. The main contribution (LF loop) at lower frequencies is relative to the a-CN_x/electrolyte interface and is strongly influenced by the dc potential. Its amplitude is equal to the transfer resistance R_t, very high at moderately negative potential (for instance -0.40 V/SCE), and much lower at a much more negative potential (for instance -1.20 V/SCE), potential at which nitrate reduction starts to occur.

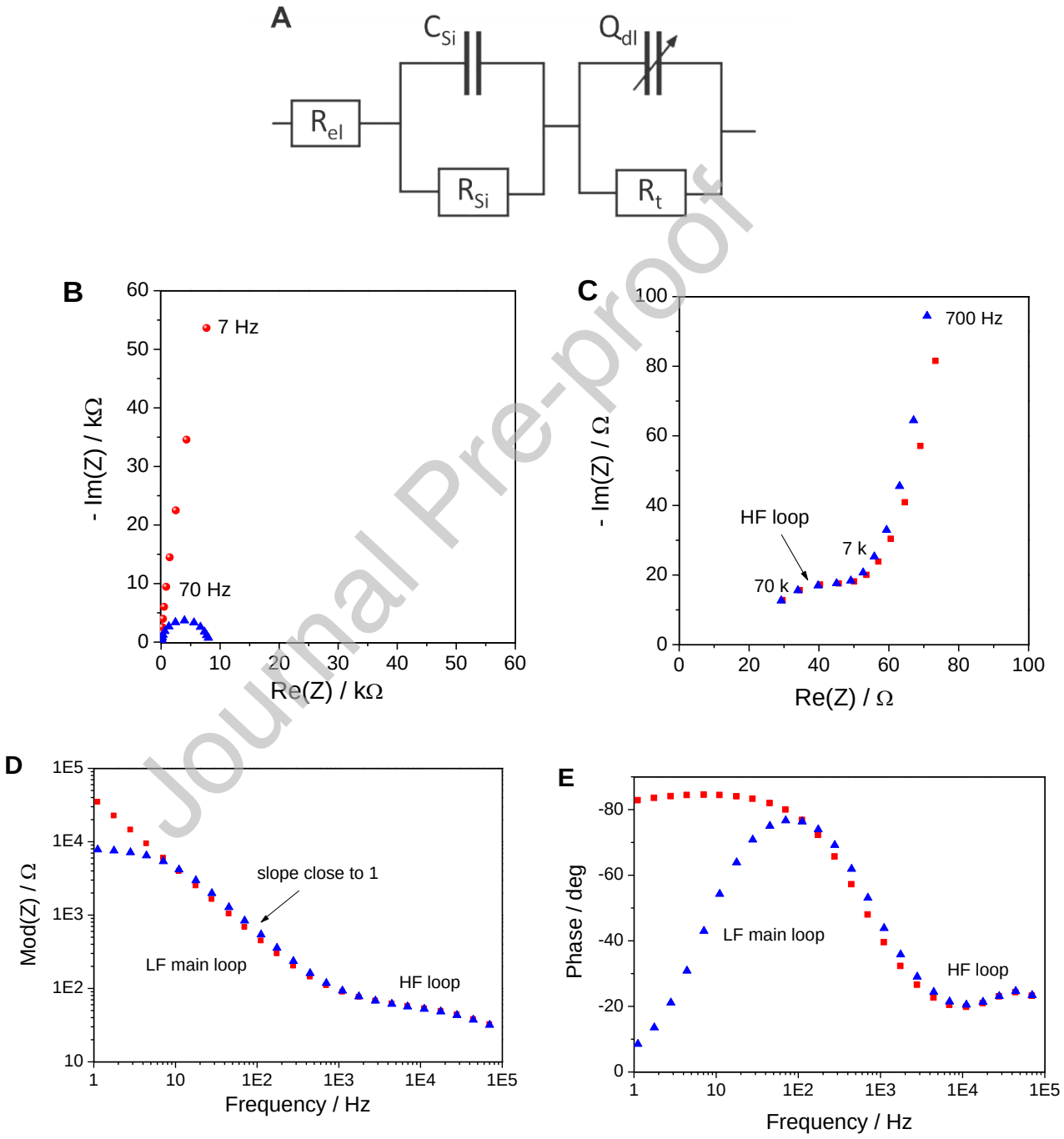

Figure 1. A) Electrical circuit used to fit the impedance data. Typical examples of the impedance spectra illustrated as Nyquist (B,C) and Bode (D,E) representations. These data correspond to the a-$CN_{0.13}$/($HClO_4$ 0.1 M + 0.01 M $NaNO_3$) system, at -0.40 V/SCE (red scatters) and -1.20 V/SCE

(blue scatters), potential at which nitrate reduction starts to occur. HF: high frequency, LF: low frequency.

RESULTS

Voltammetry

Before EIS measurements, current-voltage curves were recorded between -0.30 and -1.80 V/SCE, at a potential scan rate of 50 $mV \cdot s^{-1}$. **Figure 2A** shows a general view of the response at the a-$CN_{0.13}$ electrode in various nitrate solutions at 0.01 M in $HClO_4$ 0.1 M. From **Figure 2A** the main finding is the absence of significant reduction current in the potential domain -0.4 to -1.25 V/SCE, defining the operational domain for the EIS measurements. Actually, when looking at the µA scale, very small currents are detected, they are shown in **Figure 2B** in a logarithmic scale. When scanning the potential towards more negative values, the current response is about the same whatever the cation in the electrolyte. When scanning in the reverse sense, the situation is different, due to the effect of the structural rearrangement of the interfacial space charge, with noticeable differences according to the cation considered, for instance there is a gap of 200 mV between Li^+ (black line) and Na^+ (red line) solutions.

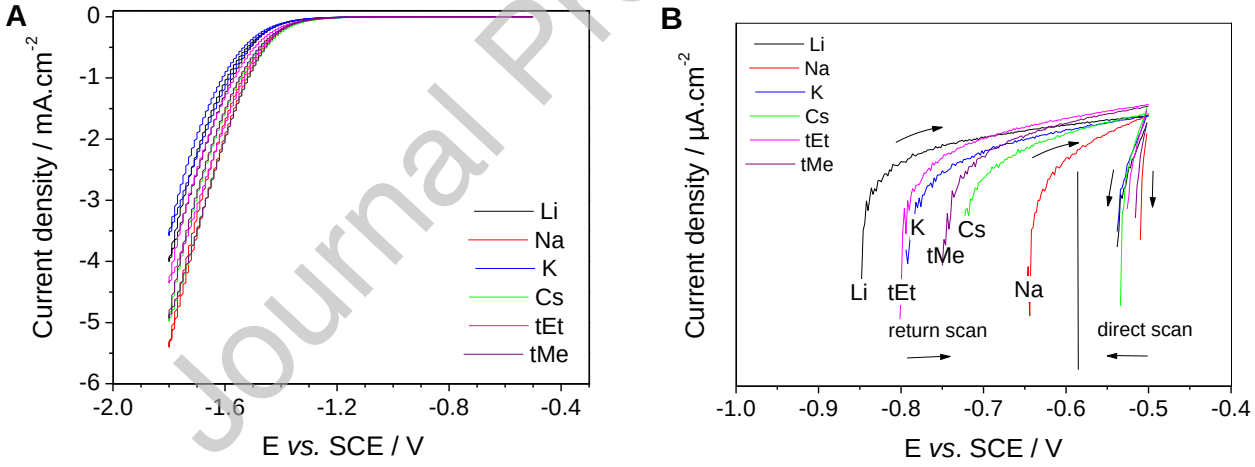

Figure 2. Current-potential response at a-$CN_{0.13}$ electrode for various nitrate solutions at the concentration 0.01 M in $HClO_4$ 0.1 M, at a potential scan rate of 10 $mV \cdot s^{-1}$. A) General view showing the absence of significant faradaic contribution in the potential domain -0.4 to -1.25 V/SCE. B) in a logarithmic scale, shows the effect of the rearrangement of the interfacial space charge upon the faradaic response, with noticeable cation-induced differences for the return scan not observed for the direct scan.

Additional information is provided by looking at the variations of the transfer resistance R_t with the potential (see **Figure S1** and **S2**). As expected, R_t is decreasing when the potential becomes more

negative and for a given potential is lower when nitrate concentration is increased. The striking point is the presence of a "break" in the slope of the R_t(E) curve possibly assigned to the potential of zero charge, as the frontier between the anion-rich to cation-rich interfacial region, around -0.9 V/SCE. This feature is well visible in the presence of small cations indicating a transition more abrupt for the latter in comparison to large cations.

Capacitance data from EIS experiments

The capacitance data between -0.40 and -1.25 V/SCE for the a-$CN_{0.13}$ electrode in aqueous $HClO_4$ 0.1 M in various conditions are gathered in **Figure 3**. In **Figure 3A**, it is seen a flat response for the supporting electrolyte, without and with 0.01 M sodium perchlorate, and a bell-shaped curve when 0.01 M sodium nitrate is present. The bell shape is also observed (**Figure 3B**) when the sodium cation is replaced by lithium or potassium one, keeping a 0.01 M concentration, with some differences in the capacitance maximum, around 6.5 $\mu F \cdot cm^{-2}$ for lithium and potassium and 8 $\mu F \cdot cm^{-2}$ for sodium salt . The effect of changing the nitrate concentration is illustrated in **Figure 3C** for sodium nitrate at 0.001, 0.01, 0.05 and 0.1 M. Whatever the concentration tested the profile is the same, the capacitance maximum increasing with the nitrate concentration, from 7 to 8.5 $\mu F \cdot cm^{-2}$. For comparison to the case of solvated small cations (Li^+, Na^+, K^+), the case of weakly solvated large cations (Cs^+, tMe^+, tEt^+) has been considered at the same concentration 0.01 M (**Figure 3D**). The response of the three large cations are superimposed with a maximum around 8 $\mu F \cdot cm^{-2}$ and a more abrupt profile at the less negative potentials than for small cations. **Figure S3** shows a Mott-Schottky representation of the interfacial capacitance evidencing a linear domain at highly negative potentials ascribed to lattice saturation effects.

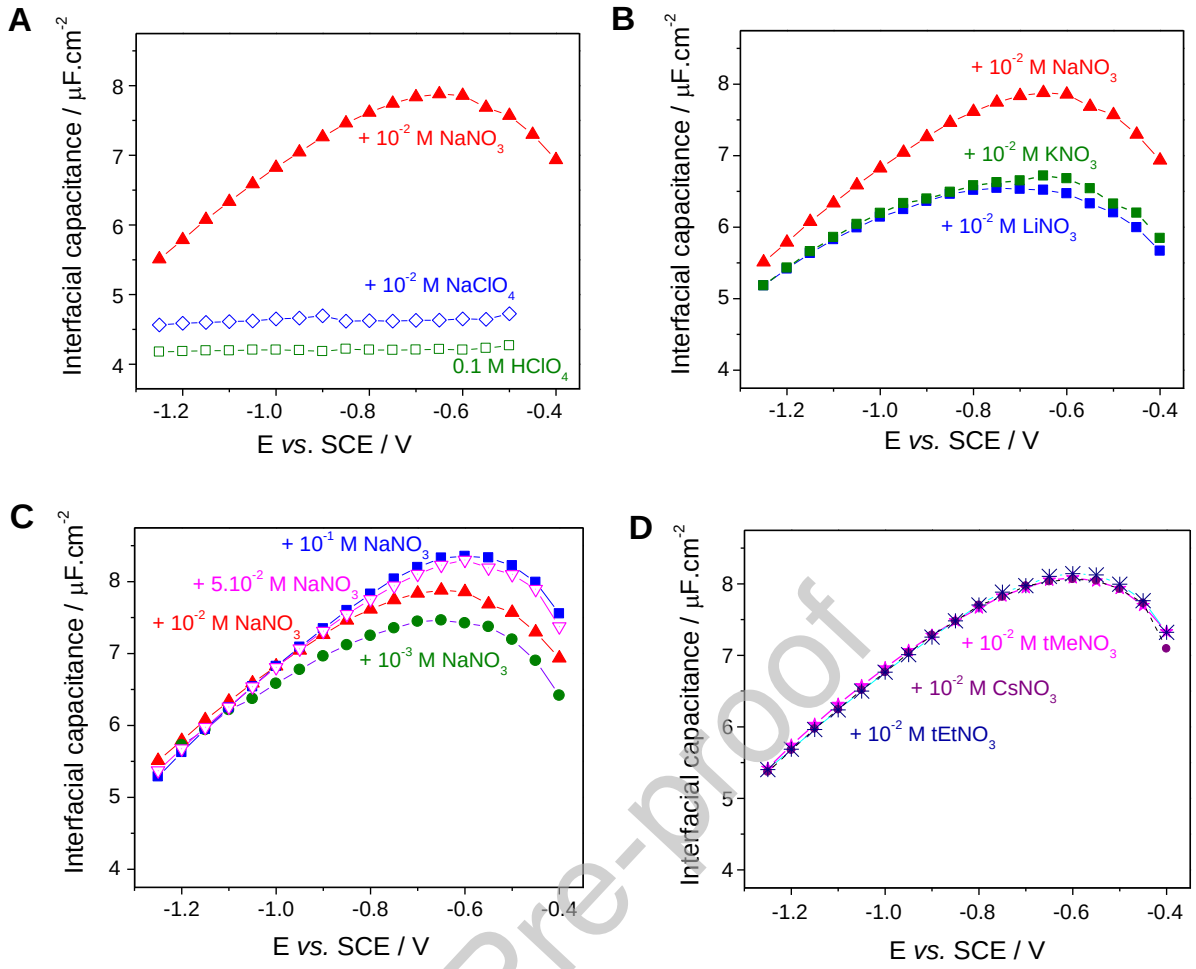

Figure 3. Capacitance *vs.* potential curves obtained for the a-$CN_{0.13}$ electrode in aqueous $HClO_4$ 0.1 M in various conditions. (A) Effect of nitrate ions on the interfacial capacitance inducing a bell-shaped behaviour. Such a behaviour is observed in the case of small solvated cations (Li^+, Na^+, K^+) depicted for the concentration 0.01 M (B), with a capacitance maximum increasing with nitrate concentration exemplified for sodium nitrate at concentrations 0.001, 0.01, 0.05 and 0.1 M (C), and in the case of large weakly solvated cations (Cs^+, tMe^+, tEt^+) at the concentration 0.01 M (D). The capacitances were calculated using **Equation 1**.

INTERPRETATION OF THE CAPACITANCE-VOLTAGE CURVES

In literature, there is a number of theoretical works for modelling a non-classical behaviour of the interfacial capacitance.[27] Among them, a few have been used to analyse experimental capacitance data. To our knowledge, it is the case for the lattice-gas model[11] and, recently, for the generalized Helmholtz model[28]. The latter was applied to the Au (100) electrode in contact with either an ionic liquid or an aqueous NaCl 1 M solution. The capacitance profiles spreading over 2-3 Volts were characterized by capacitance humps interpreted by considering the Helmholtz capacitance of the compact layer with voltage-dependent dielectric constant and thickness and assuming a negligible

contribution of the diffuse layer. Note that this approach needs molecular dynamics computations. The results presented here are characterized by a broad bell-shaped capacitance profile which substantiates the predictions in the innovative more tractable work of Kornyshev[17] and the subsequent refinement by taking into account the short-range ion-ion effects[23], formalism initially developed for ionic liquids. The semi phenomenological theory exposed in these papers provides an analytical expression involving a limited number of parameters allowing to be numerically compared to the present experimental data obtained in aqueous solutions.

This theory of the diffuse layer was treated in the frame of the lattice gas model where the volume of liquid excluded by ions is taken to be non zero as it is in the Gouy-Chapman Stern (GCS) model for ideally dilute solutions. In particular, the main result of this analytical model is featured by a bell shape or camel shape of the double layer capacitance *vs.* potential curve, the maximum being close to the point of zero charge (pzc) with a parabolic shape instead of the minimum predicted in the GCS model. One critical ingredient is a compactness factor, γ, defined as the ratio of the bulk density of ions to the maximum possible density in the double layer. This implies the presence of voids in the system opening the possibility of increased compactness in the presence of higher electric fields, *i.e.* in the double layer. The bell shape situation corresponds to $1/3 < \gamma < 1$. For $0 < \gamma < 1/3$ a camel shape is predicted, $\gamma \sim 0$ being the GCS case. In an aqueous environment, the possibility of a compact (or Helmholtz) layer in series with the diffuse layer was assumed.

The well defined capacitance peaks in the case of the a-$CN_{0.13}$ electrode in contact with different aqueous nitrate solutions can be compared to the predictions of the Kornyshev theory about the diffuse layer capacitance established at the interface between an ionic liquid and an electrode.[17,23] In the case of an a-$CN_{0.13}$ electrode, a comparison seems feasible if three points are taken into consideration. The first one is to consider that a compact layer is present at the interface characterized by a capacitance C_H of the order of a few $\mu F \cdot cm^{-2}$. The second point is a consequence of the first one, *i.e.* a potential distribution has to be taken into account at the interface, due to the series arrangement between the capacitances C_H and C_{dif} of the compact and diffuse layers respectively. C_H was assigned a sigmoid profile with different anodic and cathodic plateaus far from the pzc:

(2)

λ^{-1} represents the main potential domain where C_H varies from the anodic C_H^{anod} to the cathodic C_H^{cath} plateaus. $E_{1/2}$ marks the switching potential for C_H between the anodic and cathodic domains,

passing from C_H^{cath} to C_H^{anod}. The third point is to take into account the ion-ion short-range interactions which modify the potential actually seen by the diffuse layer. According to Kornyshev, it is characterized by a parameter β with 0⩽β⩽1, to be introduced into the expression of the diffuse layer capacitance C_{dif} and that of γ as taken out from the work of Kornyshev[23]:

(3)

with

(4)

γ_a and γ_c being assigned to the anodic and cathodic packing contributions, respectively. In this formula, *u* was a reduced potential seen by the diffuse layer:

$$u = \frac{eE}{k_B T} \tag{5}$$

In fact, the potential drop across the diffuse layer is only a fraction of the total applied potential due to the presence of the compact layer. As an approximation, it is assumed that the potential drop was shared between the compact and diffuse layers according to their respective capacitance value which led to the following definition of *u* variations:

(6)

On this basis, it was possible to build the double layer capacitance curve C_{dl}(E) numerically by iterative increments of the applied potential dE and extract the relevant parameters. This procedure was implemented using MathCad software (see Supporting information). The optimal values of every parameters were obtained by successive trial and error processes up to obtain satisfactory agreement between simulated and experimental data. Examples of the good agreement between simulated/experimental data are illustrated in **Figure 4**. The values of the relevant parameters deduced from the simulation are gathered in **Table 1** and **Table S1** (Supporting information).

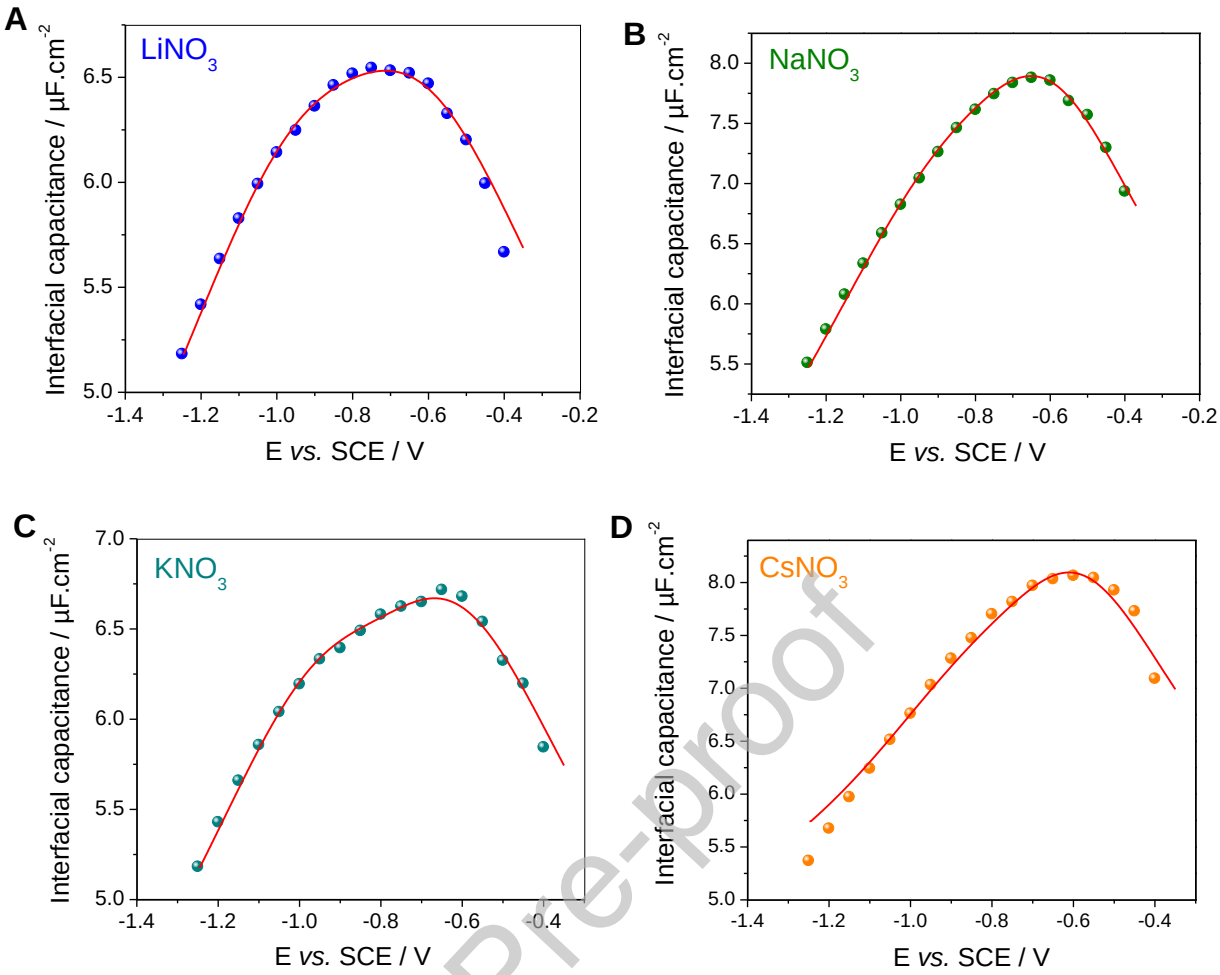

Figure 4. Examples of simulated capacitance-potential curves at the a-$CN_{0.13}$/$HClO_4$ 0.1 M interface in the presence of A) 0.01 M $LiNO_3$, B) 0.01 M $NaNO_3$, C) 0.01 M KNO_3, D) 0.01 M $CsNO_3$, according to the Kornyshev modelling (red lines).

Table 1: Parameters of the simulated interfacial capacitance – potential curves using Equations 2-6 for different nitrate salts at the concentration 0.01 M at the a-$CN_{0.13}$/$HClO_4$ 0.1 M interface.

Nitrate salt in $HClO_4$ 0.1 M	C_0 $\mu F/cm^2$	C_H^{anod} $\mu F/cm^2$	C_H^{cath} $\mu F/cm^2$	$E_{1/2}$ V/ref	λ^{-1} V	γ_a	γ_c	β
$LiNO_3$	27.9	8.6	4.8	-1.36	0.11	0.60	0.40	0.61
$NaNO_3$	29.8	11.5	3.8	-1.28	0.27	0.60	0.38	0.57
KNO_3	20.0	10.8	5.8	-1.23	0.30	0.34	0.31	0.55
$CsNO_3$	34.8	12.4	8.3	-0.71	0.25	0.50	0.40	0.84
$tMeNO_3$	36.0	12.5	8.3	-0.68	0.27	0.51	0.41	0.87
$tEtNO_3$	36.5	12.5	8.3	-0.68	0.26	0.55	0.40	0.86

In the theory, the first parameter C_o in **Table 1** is identified to the Debye capacitance C_D defined in MKSA units (ε_o = 8.84 10^{-12} F/m and e = 1.6 10^{-19} C) as:

$$C_D = \frac{\varepsilon\varepsilon_0}{L_D} \qquad \text{with} \qquad L_D = \sqrt{\frac{1}{2}\frac{\varepsilon\varepsilon_0 kT}{e\, e c_0}} \qquad (7)$$

taking $\varepsilon \approx 5$ as the dielectric constant in the interfacial region where rotational polarization is hampered by the electric field. The linear variation of $C_o \cong C_D$ predicted with the square root of the concentration c_o is effectively observed in the case of $NaNO_3$ solutions (see **Table S1** and **Figure 5A**), C_o varying from 25 µF·cm^{-2} at 0.001 M to 40 µF·cm^{-2} at 0.1 M. For the systems studied at a concentration of 0.01 M, there is a marked difference between small cations themselves (with $C_o \approx$ 20 for K^+ and around 30 µF·cm^{-2} for Li^+ and Na^+) and large ones (≈ 36 µF·cm^{-2} for Cs^+, tMe^+, tEt^+) (**Table 1**). Concerning the capacitance of the compact layer, the cathodic plateau is found systematically lower than the anodic one, suggesting a possible contribution of the anion even at cathodic overpotentials. The structural reorganisation of the compact layer is different for small and large cations. The switching potential $E_{1/2}$ is -0.7 V/SCE for the largest cations, it is much more negative for the smallest ones (-1.3 V/SCE).

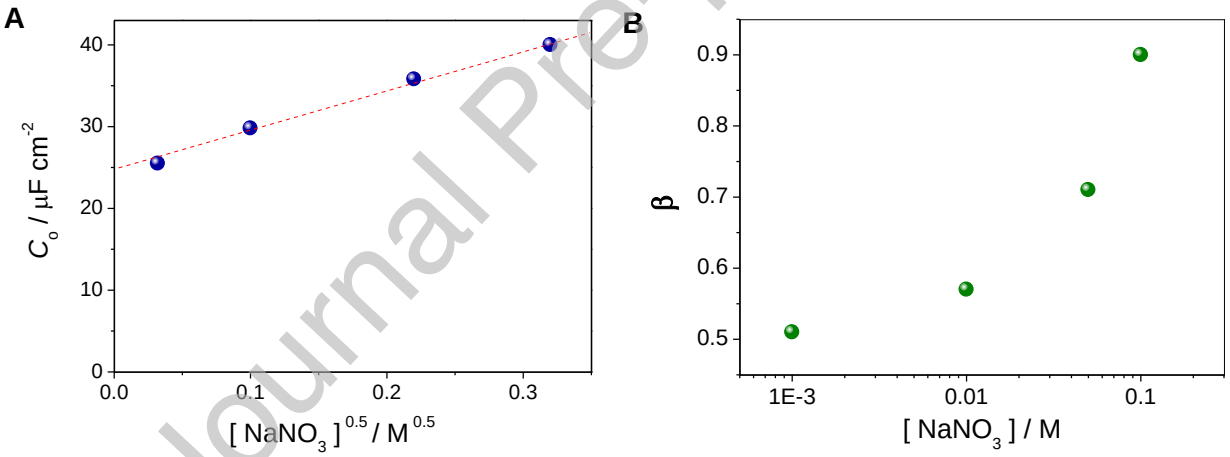

Figure 5. A) Variation of the C_o capacitance obtained by simulation with the square root of the sodium nitrate concentration, in agreement with the theoretical prediction C_o identical to C_D, the Debye capacitance. B) Variation of β with the sodium nitrate concentration.

The transition width between the anodic (cation rich) and cathodic (anion rich) regime, as measured by parameter λ^{-1}, is of the same order of magnitude (100 to 300 mV) for all the studied systems. In general, the cathodic compactness factor, γ_c, is lower than the anodic one, γ_a. For the KNO_3 solution, γ_a and γ_c are close to 0.33, this value leading to the appearance of a camel shape for the capacitance-voltage curve (see **Figure 4C**). Actually, the observed double layer capacitance is the series combination of those of the compact and diffuse regions. **Figure 6** shows typical examples of

the contributions of these two regions. The capacitance of the compact layer is about two or three times lower than that of the diffuse layer, therefore it plays a significant role in determining the values and the profile of the double layer capacitance. In the present study, the response of the diffuse layer depicts a more or less broadened bell shape. The only exceptions concern the KNO_3 solution and the less concentrated solution 10^{-3} M $NaNO_3$, for which a camel shape is evidenced for the diffuse capacitance (**Figure 6C** and **S4**), but less visible for the double layer capacitance (**Figure 3**). Such a smoothing effect arises mainly from the contribution of the compact layer capacitance, but also to the so-called "short range" factor β which tends to slow down the effect of the applied potential. From Table 1 the particular behaviour of the potassium cation by comparison with lithium and sodium ones is clear. Such a specific situation of potassium salt has already been addressed in the literature, for instance in conductivity studies[29]. The arrangement of the solvation shell of K^+ gives rise to a larger mobility and a better ability for compactness than for Li^+ and Na^+.

Concerning the "short range" factor β, it is clearly evidenced in **Table 1** that there is a marked difference between small cations (β around 0.55) and large ones (β around 0.85) for a nitrate concentration of 0.01 M. In the case of small cations, strong short range interactions are able to take place in the interfacial region as for instance ion pairing formation. These anion-cation interactions are markedly minimized for the large cations in the diffuse layer as well as for the compact layer. From **Table S1** that reports the fitting parameters for various $NaNO_3$ concentrations (from 0.001 M to 0.1 M), and **Figure 5B** one can notice that ion-ion interactions are progressively averaged when increasing the salt concentration from 0.001 M (β = 0.51) to 0.1 M (β = 0.90) without noticeable change in the compactness factors γ_a and γ_c. As mentionned in Ref 23 parameter β reflects additional difficulty to separate ions of opposite charge and this difficulty is seen to be decreased as nitrate anion concentration is increased up to 0.1 M, in relation with the coresponding decrease of the distance between nearest neighbours.

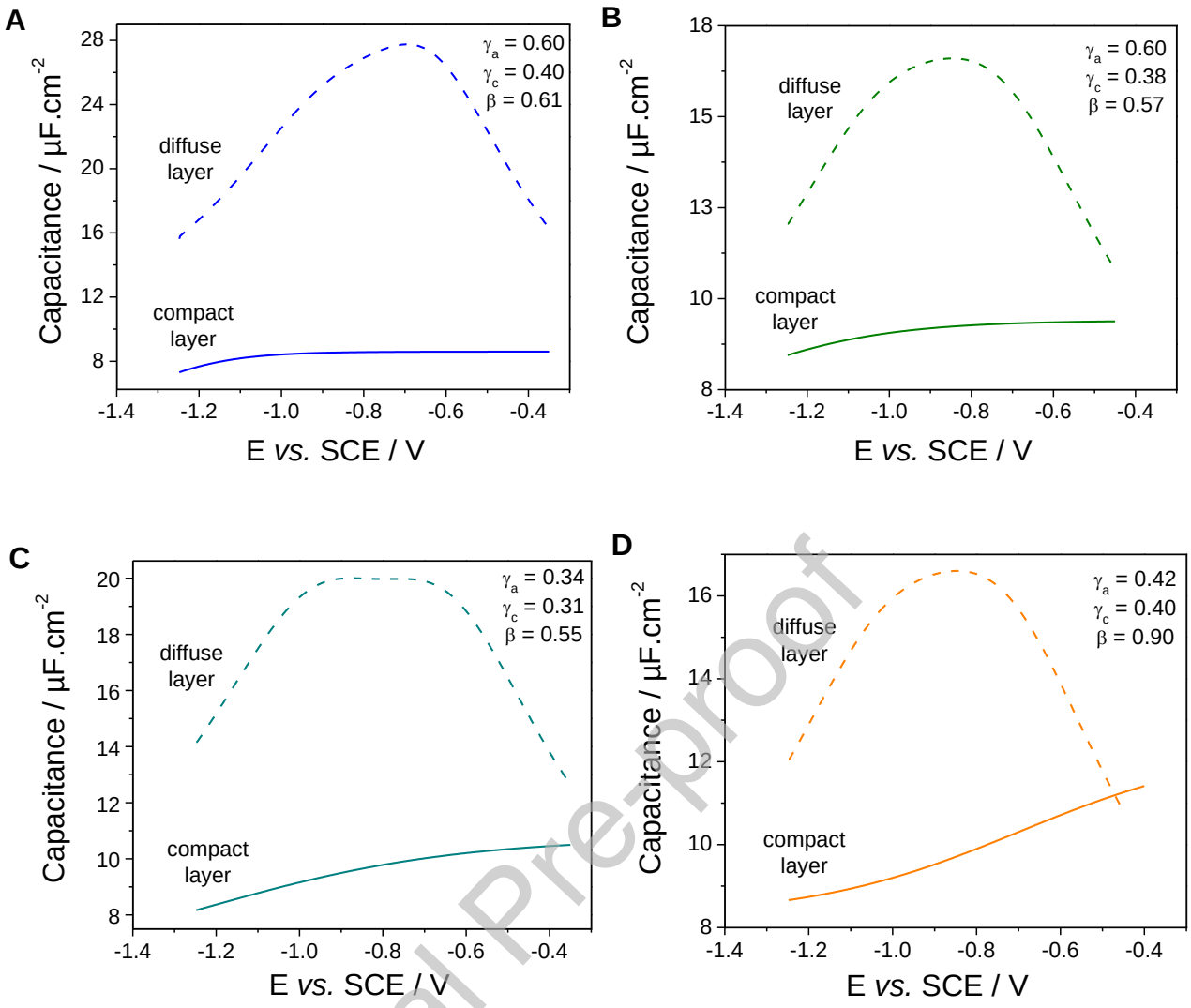

Figure 6. Compact layer and diffuse layer capacitances *versus* applied potential issued from the simulations for a-$CN_{0.13}$ electrode in (A) $LiNO_3$, (B) $NaNO_3$ (C) KNO_3 and (D) $CsNO_3$ 0.01 M in $HClO_4$ 0.1 M.

CONCLUSION

In this work, the conditions for the electrochemical reduction of nitrate anions in aqueous solutions at a-$CN_{0.13}$ thin film electrodes were studied on the basis of interfacial capacitance measurements. This electrode material, characterized by a wide potential window in water, chemical inertness, fast transfer rate for outer sphere redox reactions, was expected to be a less expensive alternative to diamond electrodes for water nitrate depollution. When deposited onto single crystal silicon substrates, a-$CN_{0.13}$ thin films were ideally obtained with a very low surface roughness, in favour of interfacial capacitance studies from a fundamental point of view. Electrochemical impedance measurements were performed in an acidic aqueous electrolyte to avoid any capacitance contribution of surface charge and in a potential domain of several hundred mV width without any

significant redox reactions. It was shown that the variations of the a-$CN_{0.13}$/aqueous solution interfacial capacitance with potential are bell-shaped in the presence of nitrate ions. By taking benefits of the theoretical work developed by Kornyshev for ionic liquids, it was possible to interpret this unexpected behaviour in an aqueous electrolyte as a structural organization of the diffuse layer, controlled by strong nitrate-cation interactions and favoured by the quasi absence of roughness of the a-$CN_{0.13}$ electrode. Thus, at the a-$CN_{0.13}$/aqueous electrolyte interface, nitrate anions are engaged into strong anion-cation interactions (ion pairing at low concentration averaged as multi-ion interactions at high concentration) especially with small sized cations, leading to nitrate anion trapping in the multilayered interfacial region with a possible negative effect on nitrate reduction. In the future, it will be of interest to check the effect of surface electrode roughness on the structural organization of the double layer.

REFERENCES

(1) Horold, S.; Vorlop, K. D.; Tacke, T.; Sell, M. Development of catalysts for a selective nitrate and nitrite removal from drinking-water. *Catalysis Today* **1993**, *17* (1-2), 21-30.

(2) de Vooys, A. C. A.; van Santen, R. A.; van Veen, J. A. R. Electrocatalytic reduction of NO_3^- on palladium/copper electrodes. *Journal of Molecular Catalysis a-Chemical* **2000**, *154*, 203-215.

(3) Swain, G. M.; Anderson, A. B.; Angus, J. C. Applications of diamond thin films in electrochemistry. *Mrs Bulletin* **1998**, *23*, 56-60.

(4) Tenne, R.; Patel, K.; Hashimoto, K.; Fujishima, A. Efficient electrochemical reduction of nitrate to ammonia using conductive diamond film electrodes. *Journal of Electroanalytical Chemistry* **1993**, *347*, 409-415.

(5) Ndao, A. N.; Zenia, F.; Deneuville, A.; Bernard, M.; Lévy-Clément, C. Effect of boron concentration on the electrochemical reduction of nitrates on polycrystalline diamond electrodes. *Diamond and Related Materials* **2000**, *9*, 1175-1180.

(6) Lévy-Clément, C.; Ndao, N. A.; Katty, A.; Bernard, M.; Deneuville, A.; Comninellis, C.; Fujishima, A. Boron doped diamond electrodes for nitrate elimination in concentrated wastewater. *Diamond and Related Materials* **2003**, *12*, 606-612..

(7) Deslouis, C.; de Sanoit, J.; Saada, S.; Mer, C.; Pailleret, A.; Cachet, H.; Bergonzo, P. Electrochemical behaviour of (111) B-Doped Polycrystalline Diamond: Morphology/surface conductivity/activity assessed by EIS and CS-AFM. *Diamond and Related Materials* **2011**, *20*, 1-10.

(8) Adamopoulos, G.; Godet, C.; Deslouis, C.; Cachet, H.; Lagrini, A.; Saidani, B. The electrochemical reactivity of amorphous hydrogenated carbon nitrides for varying nitrogen contents: the role of the substrate. *Diamond and Related Materials* **2003**, *12*, 613-617.

(9) Tamiasso-Martinhon, P.; Cachet, H.; Debiemme-Chouvy, C.; Deslouis, C. Thin films of amorphous nitrogenated carbon a-CNx: Electron transfer and surface reactivity. *Electrochimica Acta* **2008**, *53*, 5752-5759.

(10) Benchikh, A.; Debiemme-Chouvy, C.; Cachet, H.; Pailleret, A.; Saidani, B.; Beaunier, L.; Berger, M. H.; Deslouis, C. Influence of electrochemical pre-treatment on highly reactive carbon nitride thin films deposited on stainless steel for electrochemical applications. *Electrochimica Acta* **2012**, *75*, 131-138.

(11) Cannes, C.; Cachet, H.; Debiemme-Chouvy, C.; Deslouis, C.; de Sanoit, J.; Le Naour, C.; Zinovyeva, V. A. Double Layer at BuMeIm Tf2N Ionic Liquid-Pt or -C Material Interfaces. *Journal of Physical Chemistry C* **2013**, *117*, 22915-22925.

(12) Cachet, C.; Cachet, H.; Epelboin, I.; Lestrade, J.-C. Tension superficielle à l'interface mercure-solution et cinétique d'adsorption de substances organiques. *Electroanal. Chem. Interfacial*

Electrochem. **1973**, *46*, 363-373.

(13) Pajkossy, T. Impedance of rough capacitive electrodes. *J. Electroanal. Chem.* **1994**, *364*, 111-125.

(14) Kerner, Z.; Pajkossy, T. On the origin of capacitance dispersion of rough electrodes. *Electrochim. Acta* **2000**, *46*, 207-211.

(15) Schlalenbach, M.; Durmos, Y. E.; Robinson, S. A.; Tempel, H. Physicochemical mechanisms of the double-layer capacitance dispersion and dynamics: an impedance analysis. . *J. Phys. Chem. C* **2021**, *125*, 5870-5879.

(16) Hedley, J. G.; Berthoumieux, H.; Kornyshev, A. A. The dramatic effect of water structure on hydration forces and the electrical double layer, *J. Phys. Chem. C* **2023**, *127*, 8429-8447.

(17) Kornyshev, A. A. Double-layer in ionic liquids: Paradigm change? *Journal of Physical Chemistry B* **2007**, *111*, 5545-5557.

(18) Bazant, M. Z.; Storey, B. D.; Kornyshev, A. A. Double Layer in Ionic Liquids: Overscreening versus Crowding. *Physical Review Letters* **2011**, *106*, 046102.

(19) Fedorov, M. V.; Kornyshev, A. A. Ionic liquid near a charged wall: Structure and capacitance of electrical double layer. *Journal of Physical Chemistry B* **2008**, *112*, 11868-11872.

(20) Fedorov, M. V.; Kornyshev, A. A. Towards understanding the structure and capacitance of electrical double layer in ionic liquids. *Electrochimica Acta* **2008**, *53*, 6835-6840.

(21) Fedorov, M. V.; Georgi, N.; Kornyshev, A. A. Double layer in ionic liquids: The nature of the camel shape of capacitance. *Electrochemistry Communications* **2010**, *12*, 749-749.

(22) Georgi, N.; Kornyshev, A. A.; Fedorov, M. V. The anatomy of the double layer and capacitance in ionic liquids with anisotropic ions Electrostriction *vs* lattice saturation. *Journal of Electroanalytical Chemistry* **2010**, *649*, 261-267.

(23) Goodwin, Z. A. H.; Feng, G.; Kornyshev, A. A. Mean-Field Theory of Electrical Double Layer In Ionic Liquids with Account of Short-Range Correlations. *Electrochimica Acta* **2017**, *225*, 190-197.

(24) Jribi, S.; Cordoba de Torresi, S. I.; Augusto, T.; Cachet, H.; Debiemme-Chouvy, C.; Deslouis, C.; Pailleret, A. Determination of surface amine groups on amorphous carbon nitride thin films using a one step covalent grafting of a redox probe. *Electrochimica Acta* **2014**, *136*, 473-482.

(25) Benlahsen, M.; Cachet, H.; Charvet, S.; Debiemme-Chouvy, C.; Deslouis, C.; Lagrini, A.; Vivier, V. Improvement and characterization of the electrochemical reactivity of amorphous carbon nitride electrodes. *Electrochem. Commun.* **2005**, *7*, 496-499.

(26) Brug; G.J.; Van. den. Eden, A.L.G..; Sluyters-Rehbach, M.; Sluyters, J.H. The analysis of electrode impedances complicated by the presence of a constant phase element. *J. Electroanal. Chem.* **1984**, *176*, 275-295.

(27) Wu, J. Z. Understanding the Electric Double-Layer Structure, Capacitance, and Charging Dynamics. *Chemical Reviews* **2022**, *122*, 10821-10859.

(28) Park, S.; McDaniel, J. G. Generalized Helmholtz model describes capacitance profiles of ionic liquids and concentrated aqueous electrolytes. *J. Chem. Phys.* **2024**, *160*, 164709.

(29) Dorn, M., Kareth, S., Weidner, E., Petermann, M. Electrical Conductivity of Lithium, Sodium, Potassium, and Quaternary Ammonium Salts in Water, Acetonitrile, Methanol, and Ethanol over a Wide Concentration Range. *Journal of Chemical & Engineering Data* **2024**, *69*, 1493-1502.

Declaration of interests

☐ The authors declare that they have no known competing financial interests or personal relationships that could have appeared to influence the work reported in this paper.

☒ The authors declare the following financial interests/personal relationships which may be considered as potential competing interests:

Catherine Debiemme-Chouvy reports was provided by Laboratory of Electrochemical Interfaces and Systems. Catherine Debiemme-Chouvy reports a relationship with Laboratory of Electrochemical Interfaces and Systems that includes: employment. If there are other authors, they declare that they have no known competing financial interests or personal relationships that could have appeared to influence the work reported in this paper.